Kodaikanal Obs Bull (1988) 9, 177 194

SOLAR X RAY BURSTS

R R Rausaria
Department of Phy ics
Regional Engineering College
Hazratbal Srinagar Kashmir 190 006, India

Abstract

The experimental results of X ray bursts about spectral characteristics, spatial distribution and directivity measurements carried out with PVO/ISEE 3 spacecraft, imaging instruments of HXIS and Hard X ray burst spectrometers during solar Maximum Mission are briefly reviewed The observed results about the above characteristics are discussed in detail in terms of a non thermal and a thermal model It is shown that the results can be interpreted in terms of beamed thick target model in which electrons stream down to the loop foot points and produce the hard X rays through electron-ion bremsstrahlung

1 Introduction

In the optical range of the electromagnetic spectrum, solar corona can be observed only during total solar eclipse or in a normal condition with the help of a coronagraph at limb However, it is not possible to observe the corona at disk because the intensity of corona in visible light is a million fold less than that of the photosphere The situation is different if the corona is observed in X ray range of the electromagnetic spectrum In this range there is negligible contribution by the photosphere due to its low temperature thereby permitting study of the structural details of the corona at the disk during normal conditions The structural details of corona can also be studied at radio wavelengths However, the intensity of the centimeter, decimeter and meter wavelength radio waves changes in passing through corona whereas there is no such effect observed on X ray which makes this part of the electromagnetic spectrum comparatively more suitable for study on the solar corona The X ray intensity of the Sun is highly variable and ranges from 10^{-4} ergs cm^{-2} sec^{-1} for quiet Sun to several ergs cm^{-2} sec^{-1} for large flares

Solar flares are explosions in magnetised plasma and are accompanied by the release of roughly 10^{32} ergs in a short interval of less than a second This high release of energy manifests itself partly in the form of electromagnetic radiation of all range of frequencies and partly in the form of corpuscular radiation in which particles accelerated to energies in the MeV range have also been detected (Svestka, 1976) The precise nature of the acceleration mechanisms at work even today are of speculative nature Out of the complete electromagnetic spectrum emitted during a flare the study of and analysis of the hard X ray is a powerful tool for the study of various parameters characterising the incident beam of high energy electrons Solar hard X radiation with photon energies greater than 10 keV is produced in observable intensity only during a flare and show rapid changes of intensity on time scales of the order of ms to several minutes In this paper we will concentrate on the characteristics of hard X ray with energies $\geq$ 10 keV only

The X ray energy spectrum above 10 keV is in most cases consistent with a power law of the differential photon flux (Kane and Anderson 1970) The photon spectral index takes values between 2 (hard spectrum) and 8 (soft spectrum) Most frequent spectral indices are around 4 to 5 whereas very hard radiation with spectral index < 3 is extremely rare Above some critical energy of the spectrum steepens rapidly i e the spectal index increases (Kane and Anderson 1970) This may be expressed by an additional

cut off factor with power law form In some events the power law extends to several hundreds of keV (Suri et al, 1975)

The hard X radiation is believed to be mainly due to bremsstrahlung in collisions between energetic electrons and the ions of the solar atmosphere Electrons with power law energy spectrum can produce power law photon spectrum usually observed and therefore this fact was regarded as an evidence of the non thermal origin of the solar hard X rays (Takakura, 1966, Holt and Cline, 1968, Holt and Ramaty 1969) The steepening of flare X ray spectrum can be obtained in principle on a thermal basis assuming a mixture of plasma components at different temperature (Chubb, 1970, Brown Melrose and Spicer, 1979) However, a thermal interpretation is contradicted by the fact that at very high temperatures needed to explain the slope of the X ray spectrum, the thermal relaxation time is much higher than the X ray burst duration In addition Lin et al (1982) have directly observed the electron spectrum escaping out of the solar atmosphere This spectrum shows a constant spectral index in the energy range from 50 keV upto 10 MeV These extremely high electron energies and the spectral hape cannot be explained on a thermal basis Whereas the low energy electrons are believed to be more or less thermal for high energy electrons non thermal interpretation seems necessary

The spatial distribution of hard X ray sources during flares have been carried out extensively by imaging instruments on SMM satellites (Van Beck et al 1980, Hoyng et al, 1981) and to lesser extent by Hinotori spacecraft (Tsuneta et al, 1984) With the aid of instruments on SMM it was possible for the first time to investigate the location and spatial extension of hard X ray sources with a resolution of 8" corresponding to 6000 km on the solar surface These observations clearly show that X ray emission comes from the foot points, thereby emphasizing the role of thick target for X ray generation Such measurements can put to rest the existing controversy between thermal and non thermal models as well as between thick and thin target models

The vertical structure of a hard X ray source can also be obtained from observation with two or more satellites separated in heliographic longitude (Catalano and Van Allen, 1973) Such multispacecraft observations can also make important contributions to the investigation of X ray anisotropy Solar X ray bursts have been observed simultaneously by detectors aboard the international Sun Earth Explorer 3 (ISEE 3) orbiting earth, and the Pioneer venus orbitor (PVO) A rare set of circumstances on 1979 November 5 permitted valuable measurements of spatial structure of ≥ 100 keV X ray source in solar flares by PVO/ISEE-3 (Kane et al 1982) While the ISEE 3 spacecraft was at its normal location close to the Sun Earth line, the PVO spacecraft was located 132° east of the Sun Earth line During a period of about 6 hr, three successive flares occurred in Hale Plage Region 16413, located at ~ S 14°, E 35° All these flares were in full view of the PVO instruments The second flare was partially occulted by the photosphere from the PVO line of sight View angles of the two instruments on ISEE 3 and PVO were 51° 6, 47° 8 and 47° 7 and 90° 0, 94° 3 and 94° 8 respectively These observations show that the hard X ray source extended from the chromosphere/transition region upto the corona but with the most intense part of the impulsive hard X ray source located at altitudes 25,00 km (Kane et al 1982) The X ray flux ratio from the PVO/ISEE 3 has been obtained by Kane et al (1982) for the three flares on 1979 November 5 in the energy range 100 200 keV and plotted against the minimum altitude h_{min} , of the X ray source that would be observed from the PVO location As reported by Kane et al (1982), the flux ratio r decreases rapidly with the increase in minimum observable altitude h_{min} , the decrease being 50% for $h_{min} \approx 2000$ km and 90% for $h_{min} \approx 2500$ km By assuming the altitude structure of the 100 keV X ray source in the three flares to be roughly similar, Kane et al (1982) interpreted this decrease as the altitude dependence of the X ray source brightness The difference in the X ray flux observed has been explained by Kane et al (1982) in terms of partial occultation of the X ray source by the photosphere from the PVO line of sight Brown, Hayward and Spicer (1981) and Brown et al (1983) have shown that the height structure observations can be explained in terms of a thick target beam model However, in their calculations the effect of source directivity was not taken into account Also, the electron distribution was taken to be of power law

form, and dispersion in energy distribution is not included In any realistic acceleration mechanism, not all the electrons will be accelerated at 0° and it is therefore, more reasonable to take wide angular distributions of electrons at the start

The mean free path of an electron incident either at 0° (small angle) or at 60° (large angle) is the same However, the vertical distance traversed by the electron coming at 60° will be less than that coming at 0 (Secant correction) As a result this electrons at 0° penetrate deeper into the chromosphere before getting stopped as compared to those electrons which are incident at larger angles (say 60°) The flux of bremsstrahlung which depends on the density of protons will therefore be more for 0° electrons than that for 60° electrons The ratio of X ray fluxes for 60°/0° will, therefore, be a decreasing function of height Later in this paper we will show that by the inclusion of source directivity the result of the thick target model correspond well with the observations However, the spectrum is not the only criteria on which to decide between the thermal or a non thermal interpretation

Quantitative information about the velocity distribution function of electrons could be derived from the measurements of the directivity and polarization of the hard X rays Earlier indirect measurements of the directivity of hard X rays above 15 keV were carried out by various workers by studying the centre to limb variation of the frequency of occurrence of hard X ray bursts (Ohki, 1969, Pinter 1969) The best study of centre to limb variations of the hard X ray burst occurrence do not show any significant longitudinal dependence (Kane, 1984, Datlowe et al 1977) More recent work by Westrand et al (1987) shows evidence for directivity from centre to limb The direct measurements of the directivity using the spacecrafts separated in heliocentric orbit has been carried out by Kane et al (1980a) These measurements provide an opportunity to study the variation of flux ratio and directivity afresh

Several authors extensively studied the spectrum, anisotropy and polarization of solar hard X rays (Brown, 1971, Petrosian, 1973, Elwert and haug, 1971, Brown, 1972, Henoux, 1975 Langer and Petrosian, 1977, Bai and Ramaty, 1978, Leach and Petrosian, 1983) The models used in these studies vary in their assumptions regarding parameters such as direction of electron beam, pitch angle distribution of the electrons, scattering and mirroring of electrons, density of ions and Compton back scattering of X rays from the photosphere In most of the studies referred to above, either the directivity was calculated for thin target geometry or for thick target with energy and angle of the electrons centered around a mean value In some cases electron spectra in the form of power laws have been used However, as the electron beam penetrates deeper into the solar atmosphere, there will be energy dependent dispersion both in electron energy and angular distributions

In this paper we present the results of our analysis on the study of spectrum, directivity and polarization of X rays by taking into account the dispersion in electron energy and angular distributions and also seek an explanation for the flux ratio observed by Kane et al (1980b, 1982) Before we proceed to the calculation of spectrum directivity and polarization of the X rays, it is desirable to give general features of calculating the electron distributions taking dispersions into account and also present the formalism used to calculate the X ray flux

II Electron Distributions

Usually, the energy spectrum of the non thermal electrons is deduced from the measured X ray spectra and the electron energy spectrum above 10 keV is taken to be powerlaw in form We consider initially monoenergetic incident beams of electrons having energy 60, 100, 300 and 500 keV, characterised by a velocity vector $\vec{v}$ The choice of monoenergetic beams is justified by the fact that the power law shape of the distribution can be obtained by giving suitable weights to monoenergetic electrons Further, due to collisions the electron beam broadens at higher column densities and becomes a continuous distribution almost independent of the original degree of beaming at injection

However, at lower column densities near the acceleration site electron distribution are dependent on the original degree of beaming The components of v in a co ordinate system with Z axis are sin α cos ϕ, sin α sin ϕ and cos α where α is the incidence angle with respect to the vertical direction and becomes the pitch angle in the presence of a magnetic field We consider the electrons directed towards the chromosphere from the acceleration site situated in the corona, at 0°, 30° and 60° incidence angles Electron transport has been calculated as a function of column density/height in the atmo phere

We consider a fully ionized thermal plasma consisting of protons and electrons It is assumed that the relativistic electron beam will be influenced by Coloumb collisions between the beam electrons and the thermal protons and electrons Since, for chromo spheric and coronal plasma the mean free path, as determined by the minimum scattering angle, is only a fraction of a centimeter, it is not possible to treat all the mall angle deflections in a pure Monte Carlo procedure The path of electrons is therefore, divided into two parts a condensed history of the small angle scattering proce s treated analyti cally followed by Monte Carlo calculations of a single large angle collision process Details of the calculations are given in (Haug, Elwert and Rau aria, 198ɔ, Koul et al, 1985)

In the condensed history the numerous collision process with small energy losses are taken into account by mean energy loss rates If an electron traversed the distance dl in a plasma of electron proton particle density n(1), its mean loss $\overline{dE}$ of kinetic energy E by small angle scatterings, which causes a deviation between the limits $\theta_{min} \leq \theta \leq \theta_L$ is given by

$$\overline{dE} = n(1)\, dl \int_{\theta_{min}}^{\theta_L} \Delta E \frac{d\sigma}{d\theta}\, d\theta \qquad (1)$$

where

$$\Delta E = \frac{\sin^2\theta}{1 \quad \Gamma^2 \cos^2\theta} E \qquad (2)$$

$$\Gamma = \left[\frac{r \quad 1}{r \quad + 1} \right]^{\frac{1}{2}} \qquad (3)$$

This equation holds for any energy, and it refers to the laboratory system where the target electron is initially at rest For scattering of elelctrons by protons and electrons, the Born approximation is valid for electron energies $E \geq 1$ keV In this energy range the minimum scattering angle is given by

$$\theta_{min} = \frac{\hbar}{mc\,\beta\,\gamma\,D} \qquad (4)$$

where $\hbar = 2\pi\hbar$, the Planck constant; m is the rest mass of the electron, β is the velocity in units of c, γ is the lorentz factor, and D is the maximum impact parameter, which usually is taken to be the Debye length

$$D = \left[\frac{kT}{4\pi e^2 n}\right]^{\frac{1}{2}} \approx 7\left[\frac{T}{n}\right]^{\frac{1}{2}} \qquad (5)$$

Here k is the Boltzmann constant, e the electron charge, T(K) the plasma temperature, and $n(cm^{-3})$ the particle density The energy loss according to equation (1) and the mean square value of the angle depend only logarithmically on θ_{min} The results are therefore, very insensitive to the choice of θ_{min} Further, since knowledge about the temperature and density in the flare plasma is of a speculative nature, we take $D = 10(2n)^{1/3}$

The numerical value of D has been chosen to equal the Debye length for chromospheric heights

The choice of θ_L the limiting angle between the condensed history and single collision processes needs some discussion The variance of mean energy loss of an electron traversing the distance dl is given by (Bohr 1915)

$$\overline{(dE - \overline{dE})^2} = n(l)\, dl \int_{\theta_{min}}^{\theta_2} (\Delta E)^2 \frac{d\sigma}{d\theta}\, d\theta \qquad (6)$$

Approximating the energy loss according to equation (2) by $\Delta E \approx E \sin^2\theta$, and using the cross section

$$d\sigma_R = \frac{2\pi r_0^2}{\beta^4 \gamma^2} \frac{\sin\theta}{(1 - \cos\theta)^2} (1 - \beta^2 \sin^2\frac{\theta}{2})\, d\theta \qquad (7)$$

where r_0 is the classical radius of the electron, $\beta = v/c$ i the velocity of the beam electrons in unit of c, and $\gamma = (1 - \beta^2)^{-1/2}$ is the Lorentz factor, it can be seen that the variation of $\theta_L = 1^0$ is only 0 06% of the total variance ($\theta_L = \pi/4$) I or $\theta_L = 5^0$ the variance would be 1 5% Although this value is not high either, we choose $\theta_L = 1^0$, since the calculation of large angle scattering by means of the Monte Carlo method can be achieved with plausible expenditure of computer time for $\theta \geq 1^0$ Now it is possible to combine the numerous collisions with small energy losses and scattering angles $\theta_L = 1^0$ into a condensed history where only the average energy loss is taken into account In a preliminary investigation (Elwert and Rausaria, 1978), this average energy loss has been neglected compared to the energy loss by single collision $\theta \geq \theta_L$

When traversing the thermal plasma, the electron will not only lose energy continuously, but it is also deflected continuously from its original direction According to Moliere Bethe's theory (Bethe 1953), the resulting angular distribution is approximately Gaussian

$$Q_0(\theta) = \frac{2\theta}{\bar{\theta}^2} \exp\left(-\frac{\theta^2}{\bar{\theta}^2}\right) \qquad (8)$$

where

$$\int_0^\infty Q_0(\theta) d\theta = 1$$

The expression $Q(\theta)d\theta$ gives the probability of a deflection resulting from multiple scattering from the incident direction, through an angle lying between 0 and $0 + d0$ after having traversed the column density N(l)

The average column density for collisions with scattering angles between θ_L and θ_{max}, corresponding to the mean free path for large angle scattering is given by

$$\bar{N} = \frac{1}{\sigma}$$

Here σ is the total cross section given by

$$\sigma = \int_{\theta_L}^{\theta_{min}} d\sigma \approx \frac{4\pi r_0^2}{\beta^4 \gamma^2} \frac{1}{\theta_L^2} \qquad (10)$$

The larger the value of θ_L, the larger the mean angular deflection and the width of the distribution function

The aim of our computations is to calculate the energy and the angular distributions of electrons at various locations in the outer atmosphere of the Sun It is assumed that the particle density n is a function of parameter S In case of a horizontal stratification, S is the height in the atmosphere counted positively downward The initial energy and angular distribution of the electrons is given at S = 0 the location of the course of fast electrons The particle density n will be represented by the barometric law

$$n = n_0 e^{aS} \tag{11}$$

The relation between S and the path length l is $S = l \cos\theta$, where θ is the angle between electron direction and grad $\hat{n}$ We first calculate the free path l that the electron travels before undergoing the next large angle scattering (Davis 1965) Berger 1965 If an electron with energy E(S) travels with the angle θ relative to the primary direction of the electron, the vertical path l between the ith and (i+1)th collision with scattering angles $\theta \geq \theta_L$ is calculated from the probability distribution

$$A(l, S, \cos\theta) = 1 \quad \exp[-N(l, S, \cos\theta)\,\sigma] \tag{12}$$

where

$$N(l, S, \cos\theta) = \int_0^l n_0 \exp[a(S + l'\cos\theta)]\, dl' = \frac{n_0 e^{aS}}{a\cos\theta}[\exp(al\cos\theta) - 1] \tag{13}$$

is the column density along the mean free path and σ is the total cross section

Uniformly distributed random numbers $R(0 < R < 1)$ are produced by a random number generator The free path l corresponds to an event with probability R, it is determined by $R = A(l, S, \cos\theta)$ By solving this equation for l the respective free paths are determined Then the shorter of these two free paths is the free path actually traversed During the traversal of this path length l, the electron lose energy by small angle deflections and changes its direction by random angle θ, which is obtained from equation (8) using another random number C given by

$$C = \int_0^\theta Q_0(\theta)d\theta, \quad (0 < C < 1) \tag{14}$$

If the electron under consideration with the initial polar angle α_i, relative to the primary direction and the azimuthal angle ϕ_i collides with an electron or a proton at a location $S + l\cos\alpha_i$ it has the reduced energy $E(S + l\cos\alpha_i)$ according to the equation

$$E[n(l)] = G + (G^2 + 2mc^2G)^{\frac{1}{2}} \tag{15}$$

where

$$G = \frac{1}{2}\left[\frac{[E(S)]^2}{E(S) + mc^2}\; 4\pi r_0^2\, mc^2 \ln\left[\frac{\theta_L}{\theta_{min}}\right] N(l, S, \cos\alpha_i)\right] \tag{16}$$

and the new polar angle α_{i+1} is related to initial angle θ_i by the relation

$$\cos\alpha_{i+1} = \cos\alpha_i \cos\theta + \sin\alpha_i \sin\theta\cos\phi \tag{17}$$

Here ϕ is the azimuthal deflection angle, which is randomly distributed between 0 and 2π The new azimuthal angle ϕ_{i+1} is determined by

$$\sin(\phi_{i+1} - \phi_i) = \sin\frac{\sin\theta}{\sin\alpha_{i+1}} \tag{18}$$

During the following single collision of the electron with ambient electron or proton with scattering angles θ_L and θ_{max} the electron again loses energy and changes its direction Another random number is selected and used to determine the scattering angle θ from the distribution

$$D(\theta, E) = \frac{\int_{\theta_2}^{\theta} (\frac{d\sigma}{d\theta})\, d\theta}{\int_{\theta_2}^{\theta_{max}} (\frac{d\sigma}{d\theta})\, d\theta} \tag{19}$$

normalized to 1 The new polar and azimuth angles obtained after the single collisions are again determined according to equations (17) and (18) If in an e e collision the energy of the knock on electron exceeds the threshold $E_{min} = E_0/20$ this is taken into account in the distribution function of the level $(S+1, \cos\alpha_1)$ The energies of the two electron are given by $E_1 = E - \Delta E$ and $E_2 = \Delta E$ The angle θ of the knock on electron relative to the direction of the incident electron is calculated from the relativistic formula

$$\tan\theta' = \frac{2}{(\gamma+1)\tan\theta} \tag{20}$$

However, the energy lo ee caused by e p collision are negligible

We have considered electron starting at the location $S = 0$, which is taken as the acceleration site situated high up in the corona The random walk of each electron is followed towards the chromosphere until it has lost nearly its total energy i e $E < E_{min}$, where E_{min} is the 1/20th of the initial energy E_0 It turned out that for all scale heights used the results depend only on the column density

$$N(S) = \int_0^S n(s)ds$$

the number of protons/cm^2 or electrons/cm^2 within the column traversed By this procedure we determine the electron energy and angular distributions at different heights (see Haug Elwert and Rausarli, 1985 for details) The energy and angular distributions of electrons are shown in Figs 1(a,b) and 2

A similar procedure for the computation of the pitch angle and spatial distribution of energetic electrons including the effects of an ambient magnetic field has been employed by Bai (1982) Leach and Petrosian (1981) used the time independent Fokker Planck equation to determine the variation of the energy and pitch angle distribution of high energy electrons injected into a cold hydrogen plasma containing either an open or closed magnetic field structure In these investigations the injected electrons have a power law spectrum shedding little light on the dispersion of the electron distribution

III Energy Spectra and Angular Distribution of X rays

The changes in the electron energy and angular distributions result in changes into X ray energy spectrum and angular distribution The photon flux produced by electrons in a fixed direction is given by

$$J(0) = n_H \int_{1+k}^{\infty} dE\, d(\cos\alpha) \int_0^{2\pi} d\phi\, g(\alpha) \frac{d^2\sigma}{d(h\nu)d\Omega} f(E)\, v(E) \quad \text{photons cm}^{-2}\,\text{S}^{-1}\,\text{keV}^{-1} \tag{21}$$

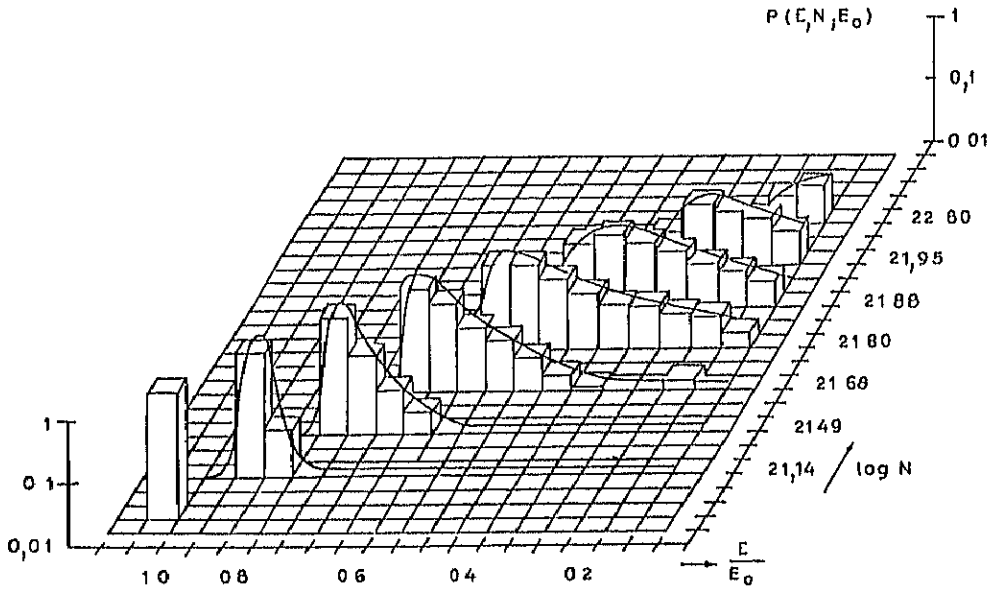

Fig.1(a) Variation of electron energy distribution with column density (No of protons/cm^2) The initial electron energy is 300 keV incident at 0°

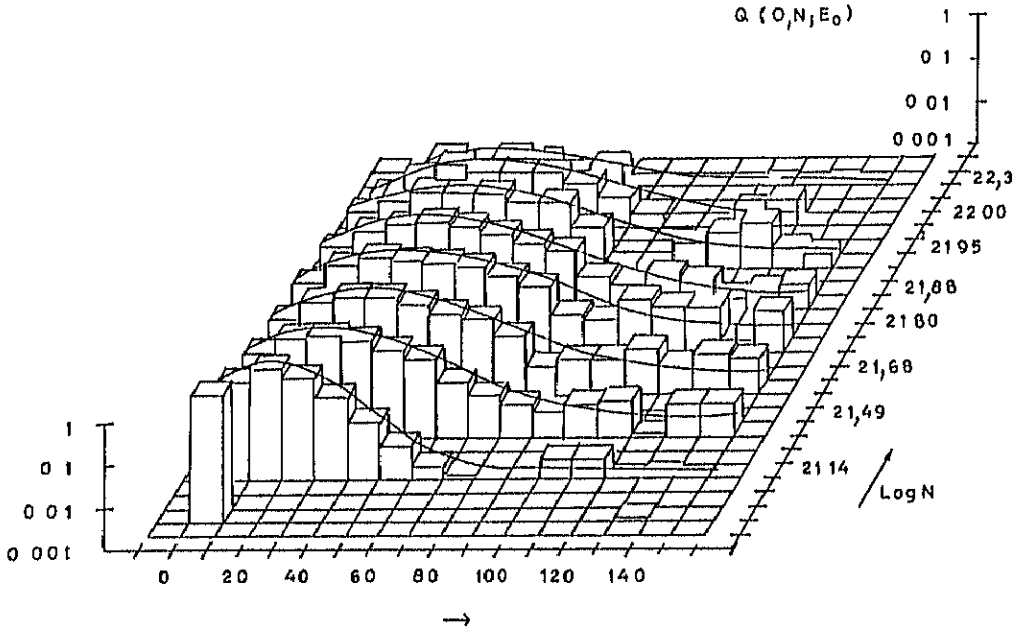

Fig.1(b) Variation of electron angular distribution with column density The initial electron enelrgy is 300 keV incident at 0°

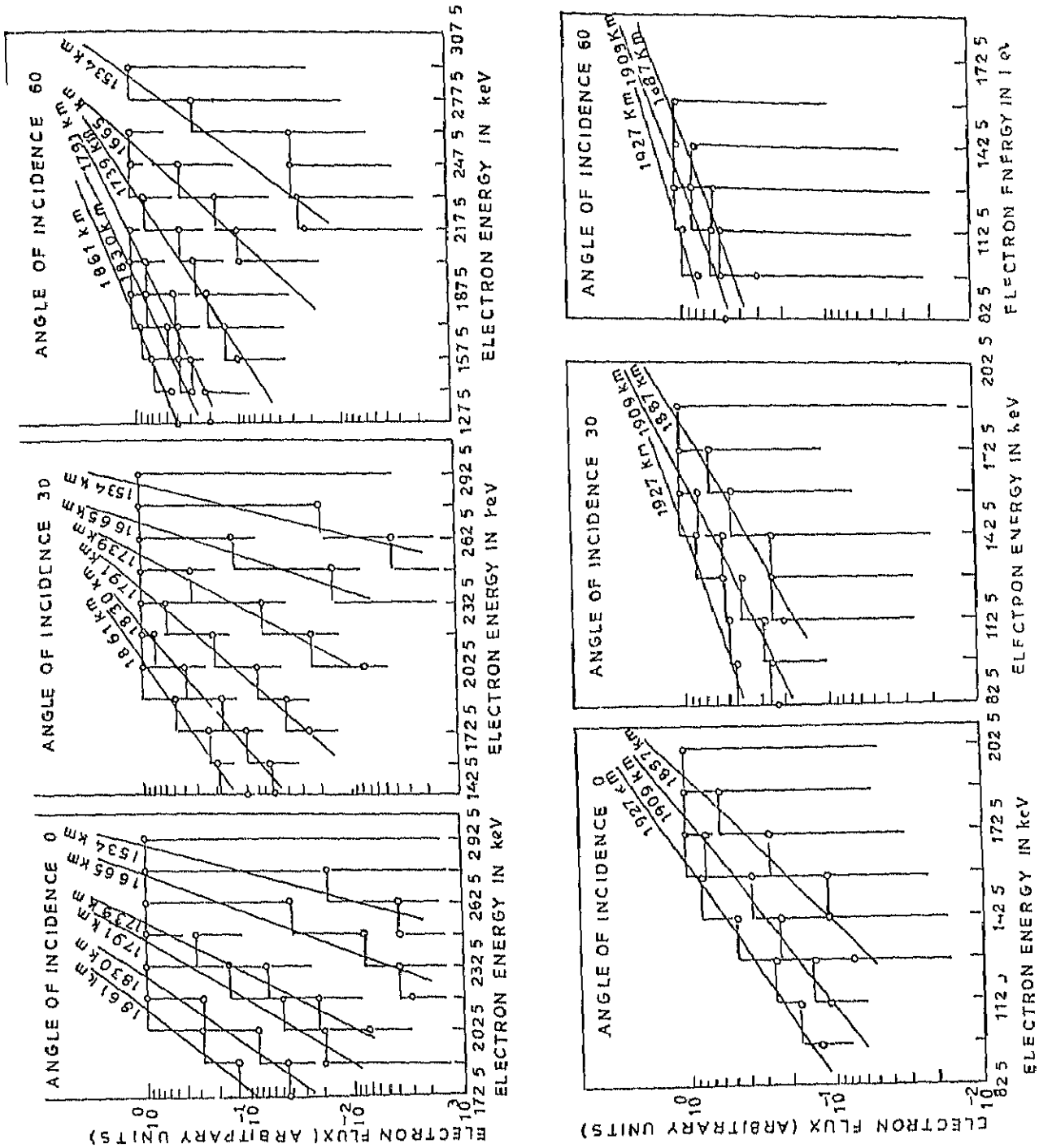

Fig.2 Variation of electron spectral index with column density The initial electron energy is 300 keV for incidence angles 0° 30° and 60°

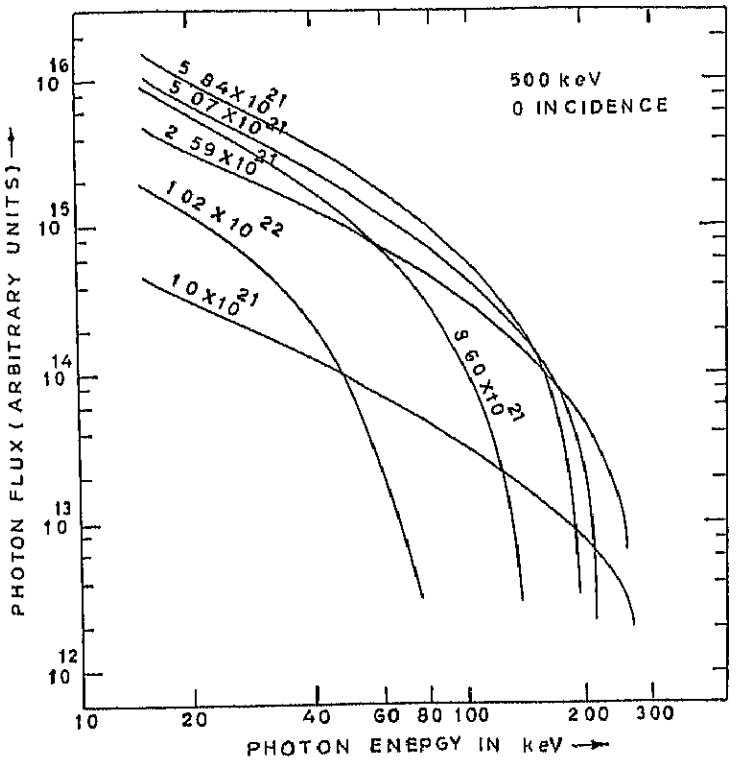

Fig.3(a) Energy spectra of X rays at various column densities (No of protons/cm^2) for a 300 keV electron beam incident at 0°

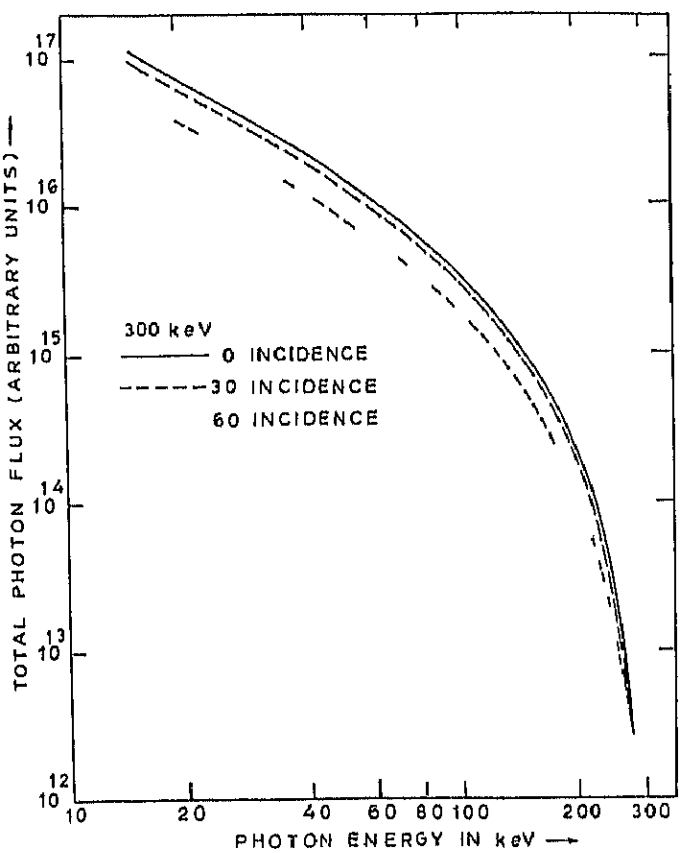

Fig 3(b) X ray flux spectra integrated over all the column densities i e spatially integrated X ray energy spectrum for a 300 keV electron beam incident at 0°, 30° and 60°

where

ϵ	is the electron energy in units of its rest mass energy mc^2
$k = h\nu/mc^2$	is the photon energy in the same units
$\frac{d^2\sigma}{d(h\nu)d\Omega}$	is the differential bremsstrahlung cross section
$g(\alpha)$	is the electron angular distribution
$f(\epsilon)$	is the electron energy distribution
$v(\epsilon)$	is the electron velocity
0	is the angle between the vertical direction and the line of sight
θ	is the angle between the electron and photon directions

In the presence of a magnetic field the electron direction will change continuously due to spiralling The angle 0 will depend on the incidence angle α, the angle θ and on the azimuth angle ϕ of the electron relative to vertical direction (magnetic field) i e

$$\cos 0 = \cos \alpha \cos \theta + \sin \alpha \sin \theta \cos \phi \qquad (22)$$

For the differential cross section the Born approximation following Sauter (1934) multiplied by the Coulomb correction (Elwert, 1939) is used in the present computation It is given in Elwert and Haug (1971) as equation (6) In this equation the second term in parenthesis should read as $(\epsilon^2 + 1 + \frac{1}{2}\epsilon' p \cos\theta)$ Integrating over all the emission angles one gets the bremsstrahlung flux as a function of energy only, at different column densities (Koul et al, 1985)

IV Results and their relation to observations

Using the bremsstrahlung cross section given in Elwert and Haug (1971) and the distribution function $f(\epsilon)$ and $g(\alpha)$ described in section II, we have computed the energy spectra (Fig 3,a,b) and angular distribution of X rays (Fig 4) for different column densities and photon energies In Fig 3a we have shown the energy spectrum at various depths in the solar atmosphere Different curves have been obtained by integrating the photon flux over the emission angles The figure clearly shows the variation in special index of the generated X rays from the lower column density (reference column density, the column density at which the dispersion in electron energy and angular distribution is insignificant) of the atmosphere to the higher column density levels As the beam of electrons injected at the top moves through the atmosphere, the number of low energy electrons increases due to the attenuation of high energy electrons with the increase in column density Thus the number of low energy photons becomes larger resulting in the progressively steeper nature of X ray spectra However, no such observation showing the spatial dependence of spectral index with column density has been reported to date In Fig 3b we plot the energy spectra integrated over all the depths i e we obtain a spatially integrated X ray energy spectrum The figure shows the variation of X ray energy spectrum for three discrete angles of electron incidence As is clear from the figure the spatially integrated X ray flux shows only a mild dependence on the electron incidence angles We further notice that the shape of calculated spatially integrated spectrum corresponds remarkably well with the observed energy spectrum obtained from PVO and ISEE 3 spacecrafts (Fig 1 of Kane et al, 1980a)

Figure 4 depicts the evolution of the X ray flux with depth as a function of emission angle for different photon energies, 10, 20, 50, 100, 150 and 200 keV The incident electron energy is 300 keV The flux is highly anisotropic at lower column densities and high energy photons show strong beaming in the forward direction i e toward the photosphere With increased column density the flux progressively tends towards isotropy Fig 4 shows that isotropization is slower for higher energies compared to low energy photons

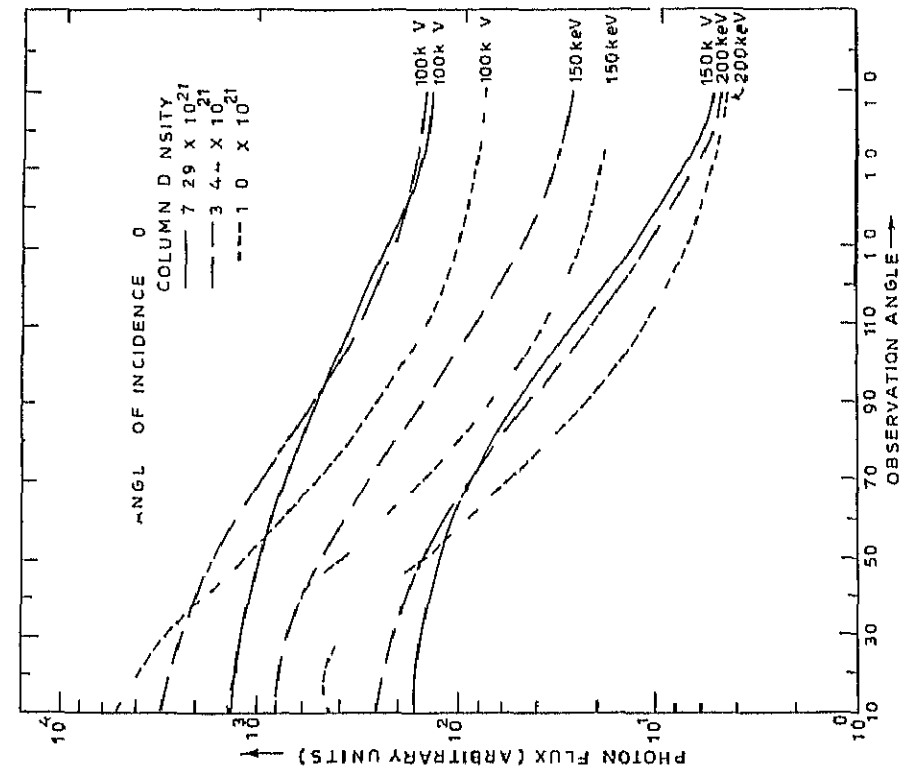

Fig.4(b) Variation of photon flux for photon energies 100 150 and 200 keV as a function of the observation angle (angle between magnetic field and direction of photon emission) at various column depths

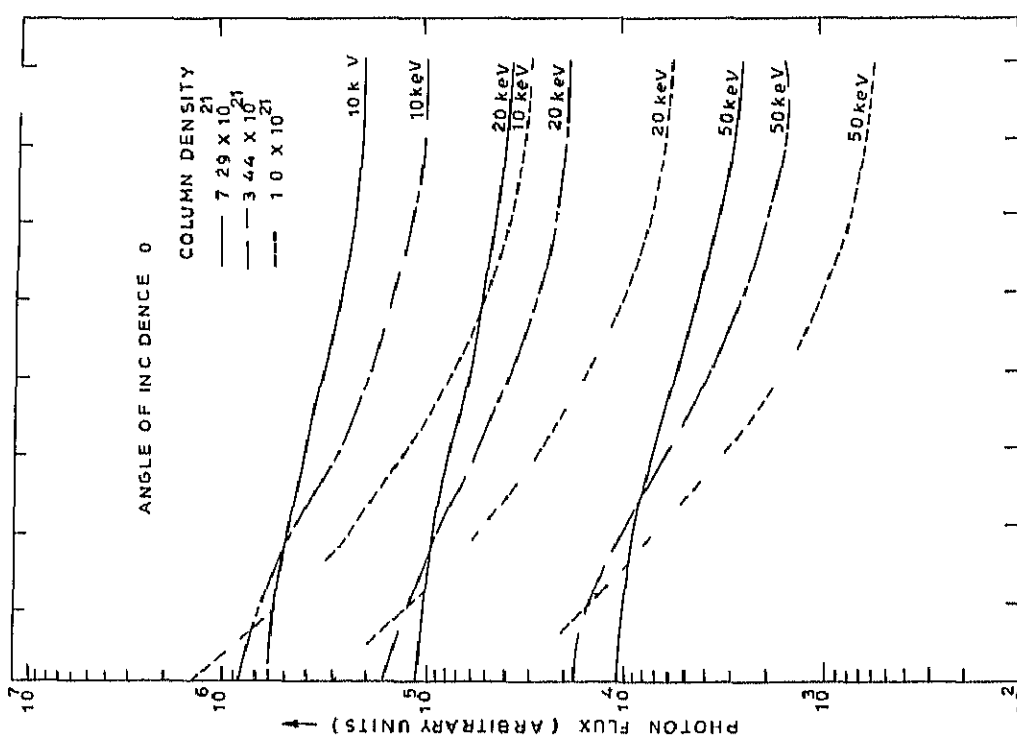

Fig.4(a) Variation of photon flux for photon energies 10 20 and 50 keV as a function of the observation angle (the angle between magnetic field and direction of photon emission) at various column depth The incident electron energy is 300 keV

Figure (2) shows that electrons incident at 60° are stopped at greater heights (lower column den ity) than those incident at 0° The ratios of the flux produced by 60° to 0° electron incidence for different photon energies are plotted in Figure 5 From the figure we find that the nature of calculated curve corresponds very well with the measured curve of Kane et al (1979) While accepting the explanation of the ob erved results put forward by kane et al (1982) in terms of photospheric absorption, we feel that the results could also be explained in terms of different incidence angles of electron beam together with attenuation at different depths in the solar atmosphere

A measure of the anisotropy A is the quotient of J_1 for $\theta_1 = 90°$ (perpendicular to the electron incident direction) to J_2 for $\theta_2 = 180°$ (opposite to the electron incidence) At higher column densities the X ray distribution (Fig 6) becomes more and more isotropic and the difference between fluxes at 90° and 180° becomes smaller To illustrate this feature we have studied the variation of the anisotropy quotient A as a function of column density in Figure 6a for photon energies 10 20, 50, 100 and 150 keV The important feature to note in this figure is that the anisotropy quotients for higher photon energies 100 and 150 keV do not have the same trend as is found for lower energy 10, 20, 50 keV photon To study the anisotropy quotient in detail we plot in figure 6b the anisotropy quotients of

(i) J_1 for $\theta_1 = 90°$ to J_2 for $\theta_2 = 150°$ i e the difference in observation/emission angle i 60°

(ii) J_1 for $\theta_1 = 90°$ to J_2 for $\theta_2 = 130°$ i e the difference in observation angle/emission angle is 40°

Comparative study of the Figure 6a and 6b gives an opportunity not only to study the variation of A with column density but also the effect of changes in the obse vation angle on the anisotropy quotient From the figures we notice that for all the angles chosen the nature of the curves remain the same However, one can see that for the lower difference angle of 40° the quotient lies between 1 and 4 and it changes less with column density than it does for difference angles above 60° where the quotient is greater than four and the fall with column density becomes progressively larger Thus, it can be inferred that with the increase in difference angle, the anisotropy quotient A becomes higher and increases more rapidly towards higher column densities

The directivity of 50 100 keV X ray emissions from solar flares have been measured with instruments on the ISEE 3 and PVO spacecraft (Fig 2 and Kane et al, 1980a) In all but three of the sight cases the difference in view angles of the two spacecraft was less than 30° but in one case it was as large as 66° The conclusion arrived at by Kane et al (1980a) favours an isotropic X ray model In order to correlate these observations with our calculations we plot in Figure 7 the flux ratio of 50 150 keV photons as a func tion of difference angle [keeping either 90° (right hand scale) or 180° (left hand scale) emission angle fixed and vary the other angle] at a fixed column density where significant dispersion of the original electron beam has already taken place From this figure we notice that the flux ratio for 50 150 keV photons is almost the same upto the difference angle of about 50°, but with the increase in difference angle beyond 60° the flux variations become significant Further for the difference angles less than 50° one would find an isotropic model, however, for the difference angles more than 60° one finds anisotropic model for X ray generation Our calculations do point toward an isotropic model for difference angles less than 60° as was observed by Kane et al, 1980a However for difference angle greater than 60° one would expect anisotropy of the X ray distributions

V Summary and Conclusions

On comparing our results with the recent observations we conclude as follows

(i) The spectral index varies along the loop (Fig 3) the spectrum is hardest at the injection site and becomes progressively softer with the increase in depth of penetration

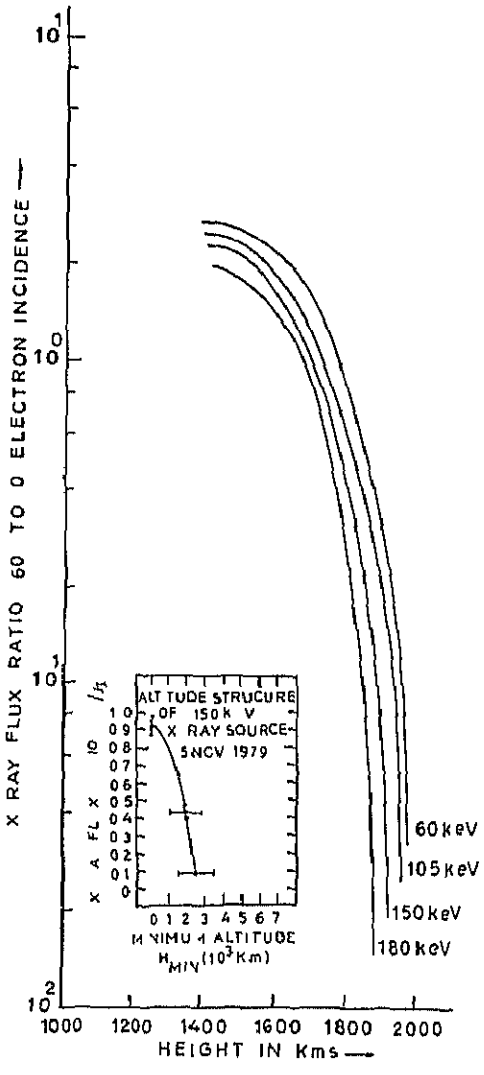

Fig.5 Variation of X ray flux ratio with height and its comparison with observations

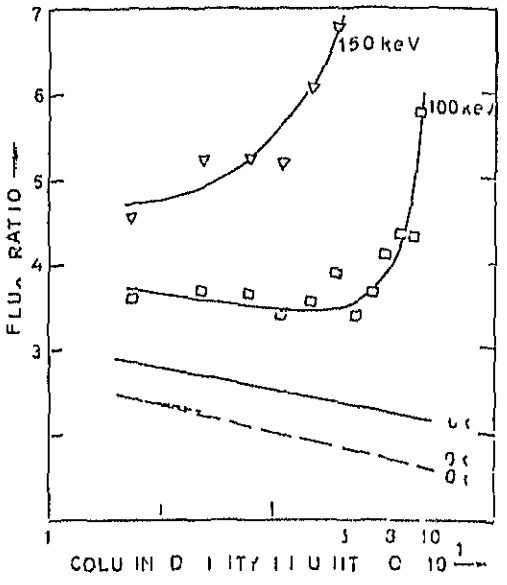

Fig.6(a) Variation of photon flux ratio or anisotropy quotient between J_1 for $O_1 = 90°$ (Perpendicular to electron incidence) to J_2 for $O_2 = 180°$ (opposite) to electron incidence with column density (No of protons/cm^2) for photon energies 10, 20, 50 100 and 150 keV and the incident electron energy 300 keV

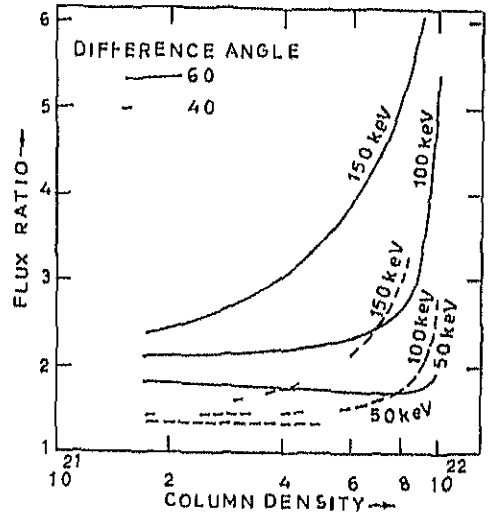

Fig 6(b) Same as Fig 6(a) but for angles $O_2 = 150°$ (Solid curves) and $O_2 = 130°$ (dashed curves) for energies 50, 100 and 150 keV The difference of angles are $O_2 - O_1$ i e 60° (solid curves) and 40° (dashed curves)

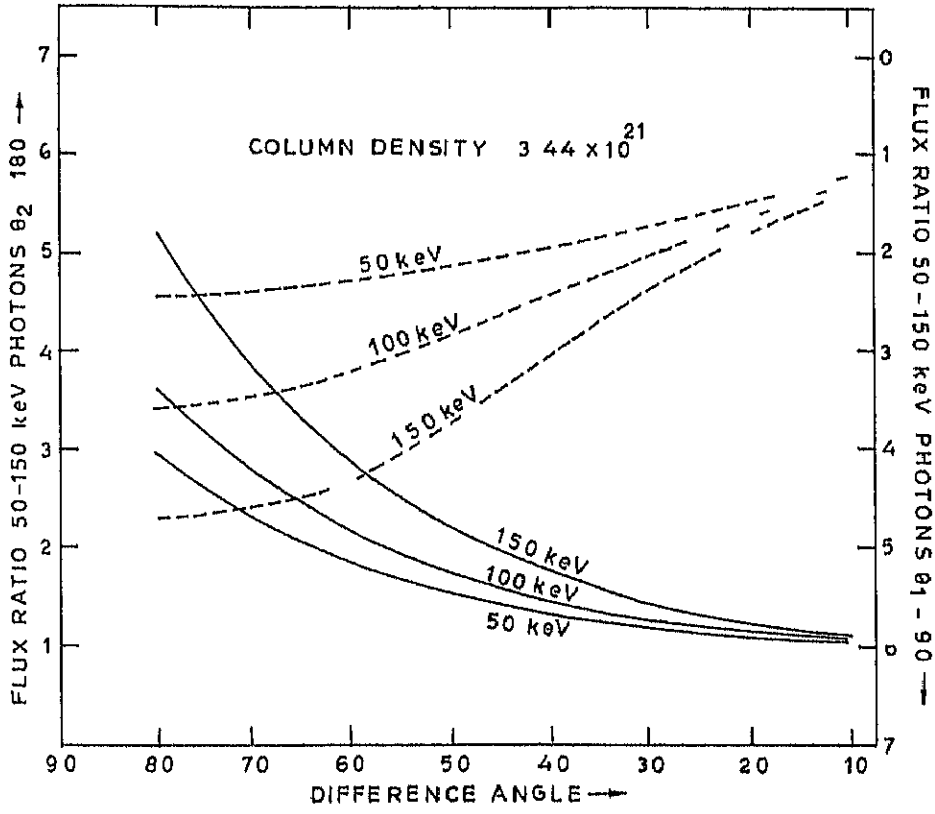

Fig.7 Ratio of 50 150 keV X ray fluxes for two different view angles O_1 to O_2 as a function of difference angles O_2 O_1 at representative column density (No of protons/cm^2) 3 44 x 10^{21} For the left hand vertical scale (curves) O_2= 180° is fixed and O_1 varies from 90° to 170° and for right hand vertical scale (curves) O_1 = 90° is fixed and O_2 varies from 100° to 170°

(higher column densities) for monoenergetic incident electrons However, in the case of power law distributions the spectrum becomes harder Thi aspect can be used to test various theories of electron acceleration Such spatial dependence of the spectral index has not been measured but the recent observations of fine time structures in X ray time profiles do reveal a harder spectra at the peak compared to that at the valley of the X ray pulse (Kane et al, 1983) By correlating the temporal and spatial peaks following the line of reasoning given by Emslie (1983), a look at our Figure 3a shows that the peak and the valley of the observed X ray pulse would be emitted from two different heights in the solar atmosphere

(ii) The integral X ray fluxes measured by ISEE 3 and PVO spacecrafts (Kane et al, 1980a, Figure 1) correspond well with our spatially integrated X ray flux Fig 3b In our calculations we have presented the picture of only one incident electron energy It has however been found that the nature of the curves remains the same over a large energy range of incident electron energies from 60 to 500 keV However, the column density at which the anisotropy ratio changes increases with increase in energy of the incident electrons The variation in photon spectra with electron incidence angle is found to be insignificant (Fig 3b)

We also find that the integrated X ray emission from the whole source has the character of the emission from a highly broadened electron beam independent of the original degree of electron beaming at the injection

(iii) The calculations of directivity of the hard X rays (Figures 6a b and 7) and their comparison with the observed directivities of the hard X rays (Kane et al, 1980a) reveals that the X ray source is almost isotropic for lower difference angles However, our calcu lations do point out that for difference angles larger than 60° one should observe aniso tropy at least at the start of the impulsive phase The inclusion of photospheric back scattering of the photon directed downwards may further reduce the anisotropy, in addition to the reduction already produced by the disper ion in electron distributions due to Coulomb collisions As shown by Bai and Ramaty (1978) the angular distribution of high energy photons are not modified significantly by Compton scattering, which indicates that there should be some observable anisotropy even after allowance for Coulomb collisions and Compton backscattering

(iv) The calculation of the anisotropy quotient as a function of column density (Fig 6a) gives some important clues regarding the electron acceleration The X ray flux ratio observed by the ISEE 3 and PVO spacecraft as a function of time (Fig 4 of Kane et al, 1982) for $\geq$ 150 keV photons shows that the ratio decreases at the start of the impulsive phase and then increases towards the end of the impulsive phase The ratio attains a fairly larger constant value during the gradual phase for approximately five minutes On comparing our calculated ratio of 100 and 150 keV photons as a function of column density (Fig 6a) with these obser vations we find that the nature of the curves is similar In the thick target geometry the high energy electrons accelerated at neutral points high in the corona and injected towards the photosphere will reach the absorption point within a fraction of a second However, the observations of Kane et al (1980a) show that the trend persists for more than 5 minutes Although it is not a general feature but if observed such long period gradual phase emissions cannot be explained unless we assume either the confinement of the particles in the magnetic field geometry injected at higher angles or a continuous injections of the electron beam The second possibility of continuous injection of the electron beams seems to be more plausible

Our calculations support X ray generation at low altitude in the thick target bremsstrahlung model (Koul et al, 1985) The energetic source electrons are most likely accelerated continuously at a neutral sheet fomed in the corona from where they propa gate downward toward the photosphere The modulation of the particles injection/accele ration and the propagation of the particles gives rise to the observed characteristic of the X ray emissions

Acknowledgements

We are thankful to Dr O N Kaul, Principal, Regional Engineering College Srinagar for his encouragement during the progress of this work The work is supported by ISRO Grant No 10/2/134

References

Bai, T 1982, in R E Lingenfelter, H S Hudson and D M Worrall (eds) γ ray transients and Related Astrophys Amer , Inst of Phys , New York p 409
Bai, T and Ramaty R 1978, Ap J 219, 705
Berger, M J 1963 Methods in computation Physics, Vol I, eds B Alder, S Fernback M Rotenberg, Academic Press, New York, p 135
Bethe, H A 1953 Phys Rev 89 1256
Bohr, N 1913 Phil, Mag 30, 581
Brown, J C 1971 Solar Physic , 25, 158
Brown, J C 1972 Solar Physics, 26, 441
Brown J C Carlaw, V A Cromwell, D and Kanne, S R 1983 Solar Phys 88, 281
Brown, J C Melrose, D B and Spicer, D S 1979 Ap J , 228 592
Chubb, T A et al 1970 Solar Physics, 13, 198
Datlowe, D W , O'Dell, S L , Peterson, L W , and Elcan, M J 1977 Ap J 212, 561
Davis, D H 1963 Methods of Computational Physics Vol I, eds B Alder, S Fernback, M Rotenberg, Academic Press, New York
Elwert, G 1939 Ann Physik 34, 178
Elwert, G , and Haug E 1971 Solar Physics, 20, 413
Elwert, G and Rausaria, R R 1978 Solar Physics, 57, 409
Emslie, A G 1983 Ap J 271 367
Haug, E , Elwert, G and Rausaria, R R 1983 Astro Ap 146, 159
Henoux, J C 1975 Solar Physics, 42, 219
Hoyng, P et al 1981, Ap J (Letters), 246 L 153
Holt, S S and Cline, T I 1968, Astrophys J 154, 1027
Holt, S S and Ramaty, R 1969, Solar Physics, 8, 119
Kane, S R and Anderson, K A 1970, Ap J 162, 1003
Kane, S R 1974 in IAU Symposium No 57, Coronal disturbances, ed G Newkirk, Jr (Dordrecht, Reidel), p 105
Kane, S R , Andeson, K A , Evans, W D , Klebesadel, R W and Laros, J 1979 Ap J (Letters), 233, L121
Kane, S R , Anderson, K A , Evans, W D , Klebesadel, R W and Laros, J G 1980a, Ap J (Letters), 239, L 85
Kane, S R et al 1980b, in Solar Flares, ed P Sturrock (Boulder University of Colorado Press), p 187
Kane, S R , Fenimore, E E , Klebesadel, R W and Laros, J G 1982 Ap J (Letters), 254, L 53
Kane, S R , Kai, K , Kosugi, T , Enome, S , Landecker, P B and McKenzie, D L 1983, Ap J 271, 376
Koul, P K , Moza, K L , Khosa, P N and Rausaria, R R 1985, Ap J 292, 725
Langer, S H and Petrosian, V 1977 Ap J 215, 666
Leach, J and Petrosian, V 1983 Sol Phys 87, 165
Lin, R P , Mewaldt, R A and Van Hollebeke, M A I 1982 Ap J 253, 949
Ohki, K 1969 Solar Phys 7, 260
Petrosian, V 1973, Ap J 186, 291
Pinter, S 1969 Solar Phys 8, 140
Sauter, F 1934, Ann Physik , 20, 404
Svestka, Z 1976 Sol Phys 47, 375
Suri, A N , Chupp, E L , Forrest, D F and Reppon, C 1975, Solar Phys 43, 415
Takakura, T 1966, Space Sci Rev 5, 80
Tsuneta, S , Takakura, T , Nita, N , Ohki, K , Tanaka, K , Makishime, K , Murakami, T , Oda, M , Ogawara, Y and Kondo, I 1984, Ap J 280, 887
Van Beck, F et al 1980, Astr Astrophys 65, 39
Vestrand, W T et al 1987, Ap J 322, 1010